Consistent Genes Associated With Structural Changes in Clinical Alzheimer's Disease Spectrum

Jinping Xu
SIAT: Shenzhen Institutes of Advanced Technology Chinese Academy of Sciences
Chao Wang
Shenzhen University
Jinhuan Zhang
Guangzhou Medical College: Guangzhou Medical University
Junjie Zhuo
Hainan University
Qingmao Hu (qm.hu@siat.ac.cn)
Institute of Biomedical and Health Engineering, Shenzhen Institutes of Advanced Technology, Chinese Academy of Sciences

Research

Keywords: Alzheimer's disease, mild cognitive impairments, gray matter volume, gene expression, enrichment analysis

Posted Date: September 21st, 2021

DOI: https://doi.org/10.21203/rs.3.rs-903119/v1

Abstract

Background:

Previous studies showed no obvious symptoms but subtle structural brain changes in a long preclinical stage of Alzheimer's disease (AD), then localized cortical and sub-cortical atrophy in MCI, and spread aggressively to nearly whole brain neurodegeneration in AD. However, the neurobiological and pathogenic substrates underlying these structural changes across AD spectrum remain largely understood.

Methods:

We obtained structural MRI imaging from ADNI datasets, including 83 early-stage mild cognitive impairments (EMCI), 83 late-stage mild cognitive impairments (LMCI), 83 AD, and 83 normal controls (NC), and aimed to explore structural changes across the full clinical AD spectrum and their genetic mechanism. Partial least square regressions and Spearman correlations were performed to explore how these changes associated with gene expression level obtained from Allen Human Brain Atlas. Finally, functional enrichment analyses were conducted using Metascape analysis to explore ontological pathways of the consistent genes.

Results:

We identified significant volume atrophy in left thalamus, left cerebellum, and bilateral middle frontal gyrus across AD spectrum. These structural changes were positively associated with gene expression levels of ABCA7, SORCS1, SORL1, PILRA, PFDN1, PLXNA4, TRIP4, and CD2AP, whereas were negatively associated with gene expression levels of CD33, PLCG2, APOE, and ECHDC3 for all three groups. Moreover, these results were verified in sub-groups of converted and stable EMCI and LMCI. Further gene enrichment analyses revealed that these positively associated genes were mainly involved in positive regulation of cellular protein localization and negative regulation of cellular component organization, whereas the negatively associated genes were mainly involved in positive regulation of iron transport.

Conclusions:

Overall, these results suggested that structural changes in prodromal and clinical AD might result from interaction of the same gene lists, which offered a better understanding of biological mechanisms underlying structural changes in prodromal and clinical AD.

Background

Mild cognitive impairment (MCI), a transitional and intermediate state between normal aging and Alzheimer's disease (AD), however, may have a significantly higher risk of converting to probable AD than normal population. The conversion rate of MCI patients to AD was at an average of 10–17% per year [1–3] and about 60% within 10 years [4]. A recent follow-up study even reported that majority (45.5%) of those MCI individuals was subsequently developed to AD for an average of 26.6 months [5]. The high

risks make it extremely important to involve early prodromal stage, especially MCI, in exploring neurobiological and pathogenic substrates of AD.

Gray matter volume (GMV) atrophy is one of main cardinal signs of neurodegeneration in AD, and is irreversible. There is a long preclinical stage of AD, in which no obvious symptoms but subtle structural changes in specific brain regions can be detected [6]. In early stage (MCI), marked localized atrophy could occur in many cortical regions and certain sub-cortical regions. During the progression from MCI to AD, global and local GMV atrophy was reported mainly in the temporal neocortex, parahippocampal cortex, and cingulate gyrus [7]. Subsequently, these atrophy spread aggressively to affect most of the brain in clinical AD [8]. Although the neurobiological and pathogenic substrates underlying particular structural changes across AD spectrum have been investigated using MRI-based genetic study, such as the associations between genetic variations within PARP1 and CARD10 and a more rapid rate of hippocampal volume loss [9, 10], between the TREM2 variant and fronto-basal grey matter loss [11], between APOE and longitudinal change in the hippocampus [12, 13], between expression level of ABCA7 and GMV changes in post-central gyrus, between superior frontal gyrus and ZCWPW1, and between right post-central gyrus and APOE [14] were identified, much more AD risk variants have been reported [15–17]. For example, a large meta-analysis on GWAS involved 74,046 people identified 20 risk genes and 11 new susceptibility loci associated with AD [18]. Since a fraction of MCI patients are in the pre-AD stages, AD risk alleles as well as that of additional genetic factors specifically influencing MCI progression have received extensive attention [19]. Indeed, some major pathogenic genes were identified in MCI using open gene expression data sets [20]. Recently, a meta-analysis also revealed several abnormally regulated genes, shared pathways, and transcription factors in MCI and AD [21]. However, one previous study identified that gene expression patterns in MCI are neither an extension of aging, nor an intermediate between aged controls and AD [22]. In Chinese population, the SORL1 genetic variants, especially polymorphism rs985421, was identified to reduce the risk of converting from MCI to AD [23, 24]. Considering these evidence, it is really important to investigate whether structural changes in the AD spectrum were driven by similar gene variants.

Recently, Allen Human Brain Atlas (AHBA, http://human.brain-map.org) microarray dataset provides an indirect way for relating brain-wide transcriptomic data to neuroimaging data [25]. The practical pipeline has been verified in various brain disorders, such as major depressive disorders [26–28], schizophrenia [29], and migraine [30]. Moreover, expression level of genes involved in mitochondrial respiration and metabolism of proteins were found to be associated with regional GMV patterns across AD-memory, AD-executive, AD language, and AD-visuospatial subgroups [31]. Therefore, it is ideal to investigate relationship between transcriptional data and GMV changes in prodromal and clinical AD using this method, which will open up a new view to advance our understanding of biological mechanisms underlying structural changes in AD.

In the current study, major steps were performed according to the schematic summary of the processing pipeline (Fig. 1): (1) GMV changes were analyzed using two sample t tests for each patient's group compared to NC; (2) gene expression levels were obtained from the AHBA data and processed using the

new pipeline; (3) regional GMV changes and regional gene expression level for interesting genes were calculated for each sample locations; (4) cross-sample spatial correlations between gene expression levels and GMV alterations were performed using partial least square regression (PLS) for each group; (5) obtain consistent genes among three group; (6) Spearman correlations between gene expression levels of consistent genes and GMV changes were performed for each group; and (7) functional enrichment analysis was conducted using Metascape analysis (https://metascape.org/gp/index.html#/main/step1) to explore ontological pathways of the consistent genes.

Materials And Methods

Participates

To ensure consistency, the Alzheimer's Disease Neuroimaging Initiative (ADNI) database (http://adni.loni.usc.edu/) was searched for normal controls (NC), early mild cognitive impairment (EMCI), late mild cognitive impairment (LMCI), and AD who were imaged at baseline using a 3 Tesla MRI scanner. Subjects were excluded if they did not have a Mini-Mental State Examination (MMSE) score, or failed image registration or segmentation. As a result, a total of 514 subjects (83 NC, 217 EMCI, 120 LMCI, and 94 AD) were remained. Since the number of subjects various very much across four groups, sub-groups of 83 EMCI, 83 LMCI, and 83 AD were randomly chosen to match age and gender of 83 NC, and were further used in the current study. Specifically, EMCI and LMCI patients were all amnestic, who were diagnosed based on the following criteria: (1) a subjective memory concern reported by themselves, their partner, or a clinician; (2) MMSE score between 24 and 30; (3) Clinical Dementia Rating (CDR) of 0.5 in the memory box; (4) cognitive and functional performance was not sufficient to diagnose as AD on the screening visit; and (5) scored 9–11 with 16 or more years of education, 5–9 for 8–15 years of education, or 3–6 for 0–7 years of education on the logical memory II subscale of the Wechsler Memory Scale-Revised for EMCI, whereas scored less than or equal to 8 for 16 or more years of education, less than or equal to 4 for 8–15 years of education, or less than or equal to 2 for 0–7 years of education for LMCI. All AD patients had to meet criteria for probable AD according to the NINCDS-ADRDA criteria, and detailed information can be referred to ADNI manual (http://adni.loni.usc.edu/wp-content/uploads/2010/09/ADNI_GeneralProceduresManual.pdf).

MRI data acquisition

Raw unprocessed 3.0 T T1-weighted MRI images were downloaded from the ADNI database, which were scanned using different MRI scanners at multi-sites. Details about data acquisition protocol can be seen in ADNI's official webpage (http://adni.loni.usc.edu/methods/documents/).

Data preprocessing

The T1 images were preprocessed using the standard pipeline in the DPABI toolbox (http://rfmri.org/dpabi) with unified segmentation and diffeomorphic anatomical registration through the exponentiated lie algebra (DARTEL). The major steps were: (1) segmenting each image into gray matter,

white matter, and cerebrospinal fluid; (2) normalization using the DARTEL; (3) resampling to a voxel size of 1.5 mm × 1.5 mm × 1.5 mm; (4) modulating by multiplying the voxel values with the Jacobian determinant derived from the spatial normalization; and (5) smoothing with a Gaussian kernel of 8 mm × 8 mm × 8 mm full-width at half maximum.

Gene expression data processing

We processed gene expression data of six postmortem adult brains using a new pipeline (https://github.com/BMHLab/AHBAprocessing) [25]. The major steps were: (1) reassigning probes to genes to the latest version using the Re-annotator toolkit (https://sourceforge.net/projects/reannotator/); (2) intensity-based filtering by a threshold of 50%; (3) selecting probes using RNA-seq data with highest correlation values; and (4) normalize expression data by scaling robust sigmoid for each participant. These procedures resulting 10,027 genes for each tissue sample. Here, we only included tissue samples from the left hemisphere since only two right hemisphere data were available in the AHBA, resulting 1285 samples.

Regional GMV differences

Two sample T-tests were performed within the gray matter mask in EMCI, LMCI, and AD patients as compared to NC to obtain voxel-wise GMV differences map using DPABI, respectively. The results were corrected using Gaussian random field (GRF, a cluster level of $p < 0.05$ and a voxel level of $p < 0.001$). Negative and positive overlap among three groups was obtained using intersection.

Moreover, spheres with a radius of 4.5 mm (i.e., 3 times of the voxel size) centered in MNI coordinate of each tissue sample (n = 1285) were draw, and regional mean T-value within this sphere were defined as the t-statistic value of GMV difference for three groups, respectively.

AD risk genes associated with GMV differences

Fifty two reproducible and established AD risk genes based on a recently published literature [32] were intersected with 10027 background genes, resulting 41 interesting genes. Then, we calculated a matrix of 1285 regions × 41 gene expressions. To further explore their relationship with GMV difference, partial least squares (PLS) regression was performed with gene expression data as predictor variables [33]. The first component of the PLS (PLS1) was further used in the current study, which was the linear combination of gene expression values that was most strongly correlated with regional changes in GMV difference. Then, cross-sample non-parametric Spearman rank was performed to determine relationship between regional PLS1 weighted gene expression and regional GMV alterations. To estimate the variability of PLS1 score for each gene, bootstrapping with 1000 times was performed. Z scores were defined as the ratio of the weight of each gene to its bootstrap standard error and ranked the genes according to their contributions to PLS1 using univariate one-sample Z tests [34]. The set of genes with Z>5 or Z< -5 were considered as positive or negative associated gene list. This procedure was performed

separately for each dataset. The final gene sets were defined as the overlap between the two datasets (interaction).

Analyses for consistent genes

Cross-sample non-parametric Spearman correlations were performed to explore relationship between gene expression level and GMV changes in each group. Moreover, the number of comparisons (n = 12) was further corrected with a significance threshold of $P < 4.16 \times 10^{-3} = 0.05/12$ (Bonferroni correction).

Re-analyses for sub-groups

Since EMCI and LMCI consist of patients who were ultimately converted to AD, remitted to NC, and stable in MCI, we subdivided them into convert (cEMCI and cLMCI), stable (sEMCI and sLMCI), and remitted sub-groups. The remitted sub-groups were relatively small, and were not included in the further analyses. Other four sub-groups (15 cEMCI, 59 sEMCI, 43 cLMCI, and 35 sLMCI) were analyzed using the same method. The weighted PLS1 scores and r values of Spearman correlation were calculated for each group.

Functional enrichment analyses

To understand pathways of gene ontology (GO) biological processes, molecular functions, cellular components, and Kyoto Encyclopedia of Genes and Genomes (KEGG) pathways, we performed Metascape analysis [35] using the positive and negative associated gene lists, respectively. The obtained enrichment pathways were thresholded for significance at 5% with at least three genes.

Results

GMV differences

Compared to NC, the EMCI patients showed significantly decreased GMV in right cerebellum, left rectal gyrus, bilateral middle frontal gyrus, as well as significantly increased GMV in bilateral calcarine and pre-central gyrus (Fig. 2A). Compared to NC, the LMCI patients showed significantly decreased GMV in right cerebellum and a wide range of regions in frontal, temporal, sub-cortical areas, as well as significantly increased GMV in bilateral calcarine and pre-central gyrus (Fig. 2B). Compared to NC, the AD patients showed significantly decreased GMV in more wide range of regions in frontal, temporal, parietal, and subcortical areas, as well as significantly increased GMV in bilateral calcarine and pre-central gyrus (Fig. 2C). After intersection, patients showed consistently decreased GMV in left thalamus, left cerebellum, and bilateral middle frontal gyrus, as well as increased GMV in bilateral calcarine and pre-central gyrus in all three groups (Fig. 2D).

Gene expressions related to GMV changes

Fifty-two AD risk genes were overlap with 10027 background genes, resulting 41 interesting genes for further analyses (Fig. 3A). We ranked the normalized weights of PLS1 based on one-sample Z tests for all 41 genes (Fig. 3B). We found that 8 genes showed significantly positive association with GMV changes

in EMCI patients, 11 genes for LMCI patients, and 11 gens for AD patients, resulting 8 genes after intersection (Fig. 3C). Moreover, 6 genes showed significantly negative association with GMV changes in EMCI patients, 7 genes for LMCI patients, and 5 gens for AD patients, resulting 4 genes after intersection. Notably, we found that the PLS1 weighted gene expression map was spatially correlated with the t-map for EMCI, LMCI, and AD (Fig. 3D).

Gene expressions related to GMV changes

For 12 consistent genes, expressions of ABCA7, SORCS1, SORL1, PILRA, PFDN1, PLXNA4, TRIP4, and CD2AP showed significantly positive associations with GMV changes, whereas as CD33, PLCG2, APOE, and ECHDC3 showed significantly negative associations (Fig. 4). Furthermore, we selected one positive and one negative gene from each dataset to present their correlation scatterplots between gene expression values and the t -statistic values of GMV changes.

Results for sub-groups

The weighted PLS1 scores and r values of Spearman correlation between 12 overlapped genes and GMV differences of cEMCI, cLMCI, sEMCI and sLMCI compared to NC were significant and extremely similar with main results (Fig. 5).

Enrichment pathways associated with GMV changes

There were two significant GO biological processes, namely positive regulation of cellular protein localization and negative regulation of cellular component organization, for positive associated genes (Fig. 6A). There was only one significant GO biological process, namely positive regulation of iron transport, for negative associated genes (Fig. 6B).

Discussion

Although GWAS, whole-exam sequencing approaches, and meta-analyses showed many AD risk genes, little was known about which genes are associated with GMV changes in AD spectrum. To narrow this gap, we explored structural changes across the full clinical AD spectrum and performed spatial correlations between these changes and expression level of AD risk genes. As a result, we identified significant volume atrophy in left thalamus, left cerebellum, and bilateral middle frontal gyrus across AD spectrum. These structural changes were consistently associated with expression levels of 12 genes for all three groups and all four sub-groups, which were mainly involved in cellular protein localization, cellular component organization, and regulation of iron transport.

As expected, we identified significantly volume atrophy in left thalamus, left cerebellum, and bilateral middle frontal gyrus across AD spectrum, which were consistent with previous studies reporting GMV reduction [7, 8]. Study suggested that GMV reduction might be associate with various micro-structural factors, such as alterations in size, morphology, and number of the cellular and non-cellular components, as well as microglial cells in cerebral cortex and sub-cortical nuclei [28]. Indeed, such micro-structural

changes were widely reported in studies on AD [36–39]. However, the genetic mechanisms resulting in these micro-structural changes as well as GMV reduction remain largely unknown. What' worse, as we known, no direct relation was identified since there is no such large sample of patients with AD who have brain-wide transcriptomic and neuroimaging data at the same time. Although it is an indirect method by assessing the similarity of spatial distribution patterns between them, our results offered a better understanding of biological mechanisms underlying structural changes in prodromal and clinical AD.

In this study, all gene expression values were positive, but the t-statistic values were negative (indicating reduced GMV) or positive (indicating increased GMV). Thus, the negative correlations indicated that brain regions with greater GMV reduction show higher gene expression, and positive correlations meant that brain regions with greater GMV reduction show lower gene expression. For instance, we identified the strongest negative association between gene expression of ECHDC3 and GMV changes, whereas the strongest positive association between gene expression of SORL1 and GMV changes across AD spectrum. The ECHDC3 is a gene that mainly encodes the enzyme enoyl-CoA hydratase domain containing 3, which has been found to be associated with brain neurodegeneration [27], especially in AD [40]. Moreover, previous study showed that the pleiotropy at ECHDC3 may be related to the association finding at this locus among persons lacking the APOE ε4 allele [41]. The SORL1, belonging to both the low-density lipoprotein receptor family and the vacuolar protein sorting-10 domain protein family [42], is a key protein involved in the processing of the amyloid-beta (Aβ) precursor protein and the secretion of the Aβ peptide [43]. It has been observed with a deficiency in the brains of patients suffering from MCI [44] and AD [45, 46], and was supported by results from meta-analyses [43]. Moreover, the SORL1 genetic variants was reported to modulate or confer risk of aMCI to probable AD in Han Chinese population [47]. Similar with our results, one study also showed that risk variants in SORL1 were associated with less gray-matter tissue in sub-cortical regions, such as putamen, thalamus, and pallidum [14].

Most importantly, the gene expression level of APOE showed significantly negative association with GMV changes across AD spectrum. However, the gene expression levels of APOE sub-types were not available in this study, which mainly included three major polymorphic alleles in humans, namely APOE2, APOE3, and APOE4. Among them, APOE4 remains by far the strongest and most prevalent genetic risk of AD since it has great influence on two hallmark pathological proteins by modulating the formation of amyloid-β peptide (Aβ) plaques and neurofibrillary tangles containing hyperphosphorylated tau protein [48]. Similar with our results, many previous studies reports significant independent effects of APOE4 genotype on hippocampal volume in MCI and AD [13, 49–51], especially in those who progressed to AD [52]. Other studies described effects of APOE4 on CA1 [53], CA3/DG [54], and subiculum [55] at sub-regional level. Mean adjusted hippocampal atrophy rates in APOE4 carriers were significantly higher in MCI converter, MCI stable, and AD compared with non-carriers [56]. In addition to hippocampal atrophy, GMV loss in temporal and parietal lobes, right caudate nucleus, insula, right parietal operculum, the right precuneus, and the cerebellum bilaterally, were also reported in APOE4 carriers in patients with MCI [57, 58]. Moreover, APOE4 has been shown to modify the association between cerebral morphology and cognitive performance in healthy middle-aged individuals [59], and between smaller volumes in the left hippocampus and a tendency to retrieve earlier acquired words in the category fluency task in MCI [60].

In addition to APOE, we also identified that gene expression level of CD33 and ECHDC3 were negatively associated with GMV changes in MCI and AD. Together, these genes were primarily involved in positive regulation of iron transport. As we all known, iron is essential for neurons and glia in many aspects [61], such as electron transport, reductase activity of nicotinamide adenine dinucleotide phosphate (NADPH), and myelination of axons. It is available to neurons and glia by transporting from the basolateral membrane of endothelial cells to cerebral compartment [62]. Although the direct relationship between brain iron and AD remains largely unknown [63], iron improper transport mechanisms are speculated to lead to the accumulation in various cortical regions and hippocampus in AD [64, 65]. Once exceeding, it might produce reactive oxygen species and pro-inflammatory proteins [66], which can't be optimally handled in MCI and AD patients [67]. Indeed, the increased iron in the brain has been considered to be one of the primary causes of neuronal death in several neurodegenerative disease, especially in AD [68]. In addition, iron is able to induce tau and Aβ aggregation [69] and enhance the toxicity of Aβ [70]. Previous AD models further support for the inter-linkage between iron metabolism and AD by showing that iron chelators may prevent neuron loss [71]. Therefore, it is reasonable to speculate that the gray matter atrophy might be related to dysregulations of iron transport, possibly iron deposit to neuron death.

Limitations

One of the major methodological limitations is worth mentioning in the current study. Specifically, gene expression level was calculated from six post-mortem brains, whereas the neuroimaging data were obtained from ADNI dataset. Moreover, we only used the gene expression data from left hemisphere since only two right hemisphere data were available in the AHBA. Therefore, a large sample across AD spectrum with both brain-wide transcriptomic and neuroimaging data of the same individuals are needed to further verify our results.

Conclusions

In conclusion, this exploratory study linked the structural changes to gene expression levels by assessing similarity of spatial distribution patterns, and showed 8/4 consistent genes positively/negatively associated with GMV alterations across AD spectrum and verified in four MCI sub-groups. These genes were mainly enriched for biological processes, and mostly involved in cellular protein localization, cellular component organization, and regulation of iron transport. Together, these results suggested that structural changes in prodromal and clinical AD might result from interaction of the same gene lists, which offered a better understanding of biological mechanisms underlying structural changes in prodromal and clinical AD.

Declarations

Ethics approval and consent to participate

Written informed consent was provided by all study participants in accordance with the Institutional Review Boards of the respective ADNI sites.

Consent for publication

Not applicable.

Availability of data and materials

T1 images of patients were downloaded from ABIDE (http://adni.loni.usc.edu/). GMV images were calculated using the standard pipeline at DPABI (http://rfmri.org/dpabi). The gene expression analysis was performed using AHBA processing pipeline (https://github.com/BMHLab/AHBAprocessing). Functional enrichments were analyzed using Metascape (https://metascape.org/gp/index.html#/main/step1). The PLS analysis was performed using codes released by Kirstie Jane (https://github.com/KirstieJane/NSPN_WhitakerVertes_PNAS2016/blob/master/SCRIPTS/).

Competing interests

The authors declare that they have no competing interests.

Fundings

This work was supported by National Natural Science Foundation of China (No. 62006220), and Shenzhen Science and Technology Research Program (No. JCYJ20200109114816594).

Author's Contributions

Qingmao Hu and Jinping Xu designed the study. Jinhuan Zhang and Junjie Zhuo downloaded the data. Jinping Xu and Chao Wang analyzed the data. Jinping Xu wrote the manuscript with help of all authors. All authors approved the final version.

Acknowledgements

No.

References

1. Petersen, R.C., et al., *Mild cognitive impairment: ten years later.* Arch Neurol, 2009. 66(12): p. 1447-55.
2. Landau, S.M., et al., *Comparing predictors of conversion and decline in mild cognitive impairment.* Neurology, 2010. 75(3): p. 230-8.
3. Davatzikos, C., et al., *Prediction of MCI to AD conversion, via MRI, CSF biomarkers, and pattern classification.* Neurobiol Aging, 2011. 32(12): p. 2322 e19-27.

4. Mitchell, A.J. and M. Shiri-Feshki, *Rate of progression of mild cognitive impairment to dementia--meta-analysis of 41 robust inception cohort studies.* Acta Psychiatr Scand, 2009. 119(4): p. 252-65.
5. Espinosa, A., et al., *A longitudinal follow-up of 550 mild cognitive impairment patients: evidence for large conversion to dementia rates and detection of major risk factors involved.* J Alzheimers Dis, 2013. 34(3): p. 769-80.
6. Tondelli, M., et al., *Structural MRI changes detectable up to ten years before clinical Alzheimer's disease.* Neurobiol Aging, 2012. 33(4): p. 825 e25-36.
7. Spulber, G., et al., *Evolution of global and local grey matter atrophy on serial MRI scans during the progression from MCI to AD.* Curr Alzheimer Res, 2012. 9(4): p. 516-24.
8. Pini, L., et al., *Brain atrophy in Alzheimer's Disease and aging.* Ageing Res Rev, 2016. 30: p. 25-48.
9. Nho, K., et al., *Whole-exome sequencing and imaging genetics identify functional variants for rate of change in hippocampal volume in mild cognitive impairment.* Mol Psychiatry, 2013. 18(7): p. 781-7.
10. Nho, K., et al., *Identification of functional variants from whole-exome sequencing, combined with neuroimaging genetics.* Mol Psychiatry, 2013. 18(7): p. 739.
11. Luis, E.O., et al., *Frontobasal gray matter loss is associated with the TREM2 p.R47H variant.* Neurobiol Aging, 2014. 35(12): p. 2681-2690.
12. Apostolova, L.G., et al., *ApoE4 effects on automated diagnostic classifiers for mild cognitive impairment and Alzheimer's disease.* Neuroimage Clin, 2014. 4: p. 461-72.
13. Andrawis, J.P., et al., *Effects of ApoE4 and maternal history of dementia on hippocampal atrophy.* Neurobiol Aging, 2012. 33(5): p. 856-66.
14. Roshchupkin, G.V., et al., *Fine-mapping the effects of Alzheimer's disease risk loci on brain morphology.* Neurobiol Aging, 2016. 48: p. 204-211.
15. Guo, X., et al., *Genome-wide significant, replicated and functional risk variants for Alzheimer's disease.* J Neural Transm (Vienna), 2017. 124(11): p. 1455-1471.
16. Lacour, A., et al., *Genome-wide significant risk factors for Alzheimer's disease: role in progression to dementia due to Alzheimer's disease among subjects with mild cognitive impairment.* Mol Psychiatry, 2017. 22(1): p. 153-160.
17. Shen, L. and J. Jia, *An Overview of Genome-Wide Association Studies in Alzheimer's Disease.* Neurosci Bull, 2016. 32(2): p. 183-90.
18. Lambert, J.C., et al., *Meta-analysis of 74,046 individuals identifies 11 new susceptibility loci for Alzheimer's disease.* Nat Genet, 2013. 45(12): p. 1452-8.
19. Moreno-Grau, S. and A. Ruiz, *Genome research in pre-dementia stages of Alzheimer's disease.* Expert Rev Mol Med, 2016. 18: p. e11.
20. Tao, Y., et al., *The Predicted Key Molecules, Functions, and Pathways That Bridge Mild Cognitive Impairment (MCI) and Alzheimer's Disease (AD).* Front Neurol, 2020. 11: p. 233.
21. Bottero, V. and J.A. Potashkin, *Meta-Analysis of Gene Expression Changes in the Blood of Patients with Mild Cognitive Impairment and Alzheimer's Disease Dementia.* Int J Mol Sci, 2019. 20(21).

22. Berchtold, N.C., et al., *Brain gene expression patterns differentiate mild cognitive impairment from normal aged and Alzheimer's disease.* Neurobiol Aging, 2014. 35(9): p. 1961-72.
23. Gao, X., et al., *SORL1 genetic variants modulate risk of amnestic mild cognitive impairment in northern Han Chinese.* Int J Neurosci, 2014. 124(4): p. 296-301.
24. Jin, C., et al., *The SORL1 polymorphism rs985421 may confer the risk for amnestic mild cognitive impairment and Alzheimer's disease in the Han Chinese population.* Neurosci Lett, 2014. 563: p. 80-4.
25. Arnatkeviciute, A., B.D. Fulcher, and A. Fornito, *A practical guide to linking brain-wide gene expression and neuroimaging data.* Neuroimage, 2019. 189: p. 353-367.
26. Anderson, K.M., et al., *Convergent molecular, cellular, and cortical neuroimaging signatures of major depressive disorder.* Proc Natl Acad Sci U S A, 2020. 117(40): p. 25138-25149.
27. Tan, M.S., et al., *Associations of Alzheimer's disease risk variants with gene expression, amyloidosis, tauopathy, and neurodegeneration.* Alzheimers Res Ther, 2021. 13(1): p. 15.
28. Ji, Y., et al., *Genes associated with gray matter volume alterations in schizophrenia.* Neuroimage, 2021. 225: p. 117526.
29. Liu, F., et al., *Altered voxel-wise gray matter structural brain networks in schizophrenia: Association with brain genetic expression pattern.* Brain Imaging Behav, 2019. 13(2): p. 493-502.
30. Eising, E., et al., *Gene co-expression analysis identifies brain regions and cell types involved in migraine pathophysiology: a GWAS-based study using the Allen Human Brain Atlas.* Hum Genet, 2016. 135(4): p. 425-439.
31. Groot, C., et al., *Differential patterns of gray matter volumes and associated gene expression profiles in cognitively-defined Alzheimer's disease subgroups.* Neuroimage Clin, 2021. 30: p. 102660.
32. Lancour, D., et al., *Analysis of brain region-specific co-expression networks reveals clustering of established and novel genes associated with Alzheimer disease.* Alzheimers Res Ther, 2020. 12(1): p. 103.
33. Abdi, H. and L.J. Williams, *Partial least squares methods: partial least squares correlation and partial least square regression.* Methods Mol Biol, 2013. 930: p. 549-79.
34. Morgan, S.E., et al., *Cortical patterning of abnormal morphometric similarity in psychosis is associated with brain expression of schizophrenia-related genes.* Proc Natl Acad Sci U S A, 2019. 116(19): p. 9604-9609.
35. Zhou, Y., et al., *Metascape provides a biologist-oriented resource for the analysis of systems-level datasets.* Nat Commun, 2019. 10(1): p. 1523.
36. Davies, D.S., et al., *Microglia show altered morphology and reduced arborization in human brain during aging and Alzheimer's disease.* Brain Pathol, 2017. 27(6): p. 795-808.
37. Gasparoni, G., et al., *DNA methylation analysis on purified neurons and glia dissects age and Alzheimer's disease-specific changes in the human cortex.* Epigenetics Chromatin, 2018. 11(1): p. 41.
38. Ishunina, T.A., I.N. Bogolepova, and D.F. Swaab, *Increased Neuronal Nuclear and Perikaryal Size in the Medial Mamillary Nucleus of Vascular Dementia and Alzheimer's Disease Patients: Relation to*

Nuclear Estrogen Receptor alpha. Dement Geriatr Cogn Disord, 2019. 47(4-6): p. 274-280.

39. Nicastro, N., et al., *Gray matter changes related to microglial activation in Alzheimer's disease.* Neurobiol Aging, 2020. 94: p. 236-242.
40. Desikan, R.S., et al., *Polygenic Overlap Between C-Reactive Protein, Plasma Lipids, and Alzheimer Disease.* Circulation, 2015. 131(23): p. 2061-2069.
41. Jun, G.R., et al., *Transethnic genome-wide scan identifies novel Alzheimer's disease loci.* Alzheimers Dement, 2017. 13(7): p. 727-738.
42. Lane, R.F., et al., *Diabetes-associated SorCS1 regulates Alzheimer's amyloid-beta metabolism: evidence for involvement of SorL1 and the retromer complex.* J Neurosci, 2010. 30(39): p. 13110-5.
43. Campion, D., C. Charbonnier, and G. Nicolas, *SORL1 genetic variants and Alzheimer disease risk: a literature review and meta-analysis of sequencing data.* Acta Neuropathol, 2019. 138(2): p. 173-186.
44. *<Neuronal LR11sorLA expression is reduced in mild cognitive impairment.pdf>.*
45. *<SorLA expression is reduced in sporadic Alzheimer disease but not in familial Alzheimer disease.pdf>.*
46. Shen, L., et al., *Genetic analysis of quantitative phenotypes in AD and MCI: imaging, cognition and biomarkers.* Brain Imaging Behav, 2014. 8(2): p. 183-207.
47. *<SORL1 gene, plasma biomarkers, and the risk of Alzheimer's disease for the Han Chinese population in Taiwan.pdf>.*
48. Serrano-Pozo, A., S. Das, and B.T. Hyman, *APOE and Alzheimer's disease: advances in genetics, pathophysiology, and therapeutic approaches.* The Lancet Neurology, 2021. 20(1): p. 68-80.
49. Wang, X., et al., *Apolipoprotein E epsilon4 Modulates Cognitive Profiles, Hippocampal Volume, and Resting-State Functional Connectivity in Alzheimer's Disease.* J Alzheimers Dis, 2015. 45(3): p. 781-95.
50. Saeed, U., et al., *APOE-epsilon4 associates with hippocampal volume, learning, and memory across the spectrum of Alzheimer's disease and dementia with Lewy bodies.* Alzheimers Dement, 2018. 14(9): p. 1137-1147.
51. Veldsman, M., et al., *The human hippocampus and its subfield volumes across age, sex and APOE e4 status.* Brain Commun, 2021. 3(1): p. fcaa219.
52. Fang, Y., et al., *Evaluation of hippocampal volume and serum brain-derived neurotrophic factor as potential diagnostic markers of conversion from amnestic mild cognitive impairment to Alzheimer disease: A STROBE-compliant article.* Medicine (Baltimore), 2019. 98(30): p. e16604.
53. Kerchner, G.A., et al., *APOE epsilon4 worsens hippocampal CA1 apical neuropil atrophy and episodic memory.* Neurology, 2014. 82(8): p. 691-7.
54. Mueller, S.G. and M.W. Weiner, *Selective effect of age, Apo e4, and Alzheimer's disease on hippocampal subfields.* Hippocampus, 2009. 19(6): p. 558-64.
55. Donix, M., et al., *Family history of Alzheimer's disease and hippocampal structure in healthy people.* Am J Psychiatry, 2010. 167(11): p. 1399-406.

56. Manning, E.N., et al., *APOE epsilon4 is associated with disproportionate progressive hippocampal atrophy in AD.* PLoS One, 2014. 9(5): p. e97608.
57. Goni, J., et al., *Selective brain gray matter atrophy associated with APOE epsilon4 and MAPT H1 in subjects with mild cognitive impairment.* J Alzheimers Dis, 2013. 33(4): p. 1009-19.
58. Spampinato, M.V., et al., *Apolipoprotein E and gray matter volume loss in patients with mild cognitive impairment and Alzheimer disease.* Radiology, 2011. 258(3): p. 843-52.
59. Cacciaglia, R., et al., *APOE-epsilon4 risk variant for Alzheimer's disease modifies the association between cognitive performance and cerebral morphology in healthy middle-aged individuals.* Neuroimage Clin, 2019. 23: p. 101818.
60. Venneri, A., et al., *The neuroanatomical substrate of lexical-semantic decline in MCI APOE epsilon4 carriers and noncarriers.* Alzheimer Dis Assoc Disord, 2011. 25(3): p. 230-41.
61. Reinert, A., et al., *Iron concentrations in neurons and glial cells with estimates on ferritin concentrations.* BMC Neurosci, 2019. 20(1): p. 25.
62. McCarthy, R.C. and D.J. Kosman, *Mechanisms and regulation of iron trafficking across the capillary endothelial cells of the blood-brain barrier.* Front Mol Neurosci, 2015. 8: p. 31.
63. Tripathi, A.K., et al., *Transport of Non-Transferrin Bound Iron to the Brain: Implications for Alzheimer's Disease.* J Alzheimers Dis, 2017. 58(4): p. 1109-1119.
64. Mezzaroba, L., et al., *The role of zinc, copper, manganese and iron in neurodegenerative diseases.* Neurotoxicology, 2019. 74: p. 230-241.
65. Li, L.B., et al., *Iron Exposure and the Cellular Mechanisms Linked to Neuron Degeneration in Adult Mice.* Cells, 2019. 8(2).
66. Yauger, Y.J., et al., *Iron accentuated reactive oxygen species release by NADPH oxidase in activated microglia contributes to oxidative stress in vitro.* J Neuroinflammation, 2019. 16(1): p. 41.
67. Mills, E., et al., *Mechanisms of brain iron transport: insight into neurodegeneration and CNS disorders.* Future Med Chem, 2010. 2(1): p. 51-64.
68. Lu, L.N., et al., *Expression of Iron Transporters and Pathological Hallmarks of Parkinson's and Alzheimer's Diseases in the Brain of Young, Adult, and Aged Rats.* Mol Neurobiol, 2017. 54(7): p. 5213-5224.
69. Sayre, L.M., et al., *In situ oxidative catalysis by neurofibrillary tangles and senile plaques in Alzheimer's disease: a central role for bound transition metals.* J Neurochem, 2000. 74(1): p. 270-9.
70. Squitti, R., *Metals in Alzheimer's disease: a systemic perspective.* Front Biosci (Landmark Ed), 2012. 17: p. 451-72.
71. Ward, R.J., D.T. Dexter, and R.R. Crichton, *Neurodegenerative diseases and therapeutic strategies using iron chelators.* J Trace Elem Med Biol, 2015. 31: p. 267-73.

Table

Table 1
Data characteristics.

Clinical characteristics	AD	LMCI	EMCI	NC	P value[a]
Subjects	83	83	83	83	-
Age (mean ± SD)	75.39 ± 7.16	75.20 ± 6.3	76.06 ± 5.91	75.92 ± 5.73	0.787
Gender(male/female)	39/44	38/45	38/45	38/45	0.998
MMSE scores	21.49 ± 3.52	26.81 ± 2.56	27.79 ± 1.57	29.24 ± 0.89	< 0.001

Abbreviations: AD, Alzheimer's disease, LMCI, late mild cognitive impairment; EMCI, early mild cognitive impairment; NC, normal controls; SD, standard deviation; and MMSE, mini-mental state examination. [a] represents one-way analysis of variance(ANOVA).

Figures

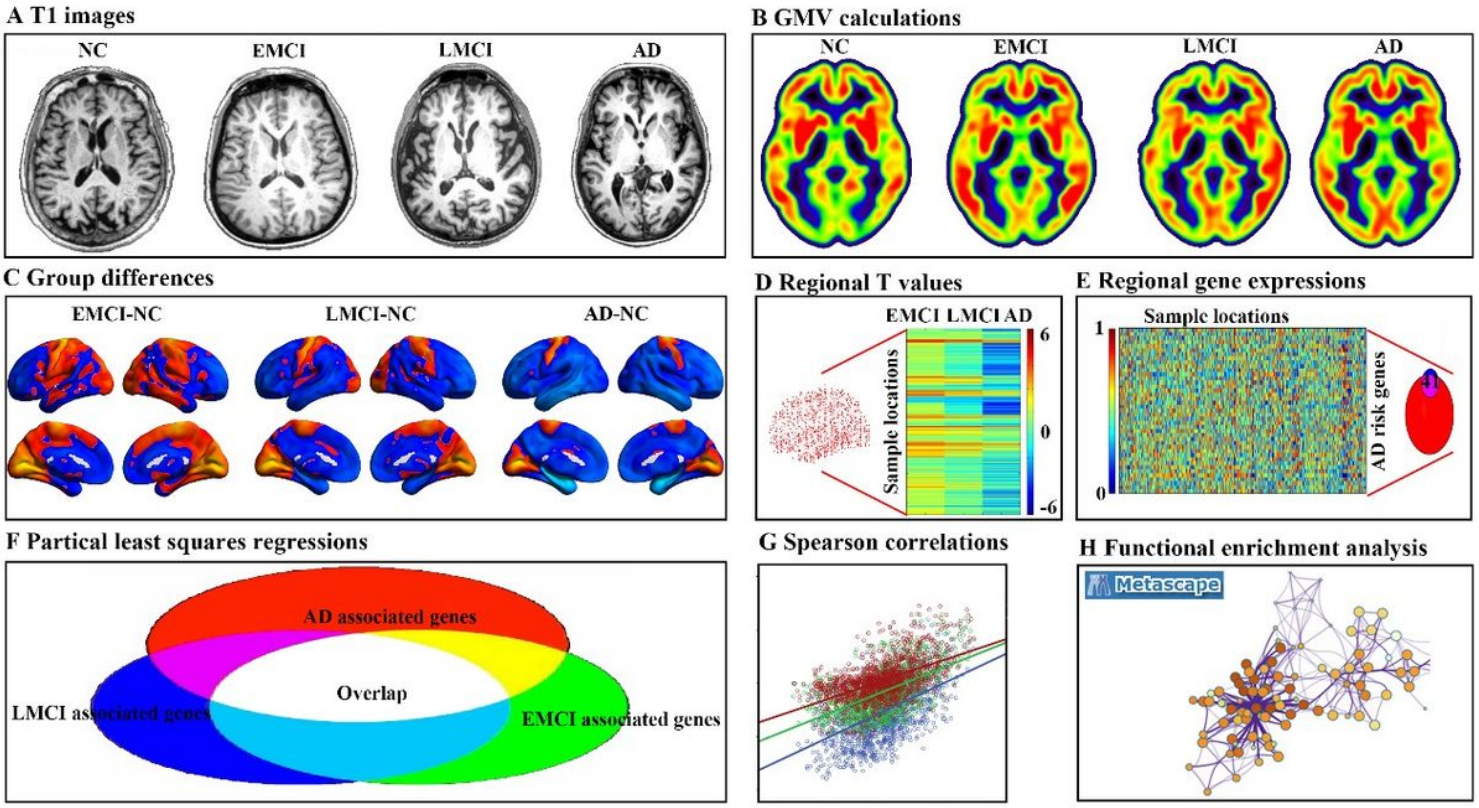

Figure 1

Pipeline of data processing. (A) Example T1 image for normal controls (NC), early mild cognitive impairment (EMCI), late mild cognitive impairment (LMCI), and Alzheimer's disease (AD). (B) Gray matter volume (GMV) for each example. (C) Two sample t-tests were used to obtain voxel-wise GMV difference between EMCI, LMCI, AD and NC. (D) Regional T value for each tissue sample in the left hemisphere. (E) Gene expression values of AD risk genes in tissue samples were obtained in six donated brains from the

Allen Human Brain Atlas. (F) Gene-wise cross-sample partial least squares (PLS) regressions were performed between gene expression and GMV differences, respectively. The intersected genes were defined as genes associated with GMV alterations for all three groups. (G) Spearman correlations between gene expression levels of overlap genes and regional GMV difference. (H) Functional enrichment analysis using Metascape.

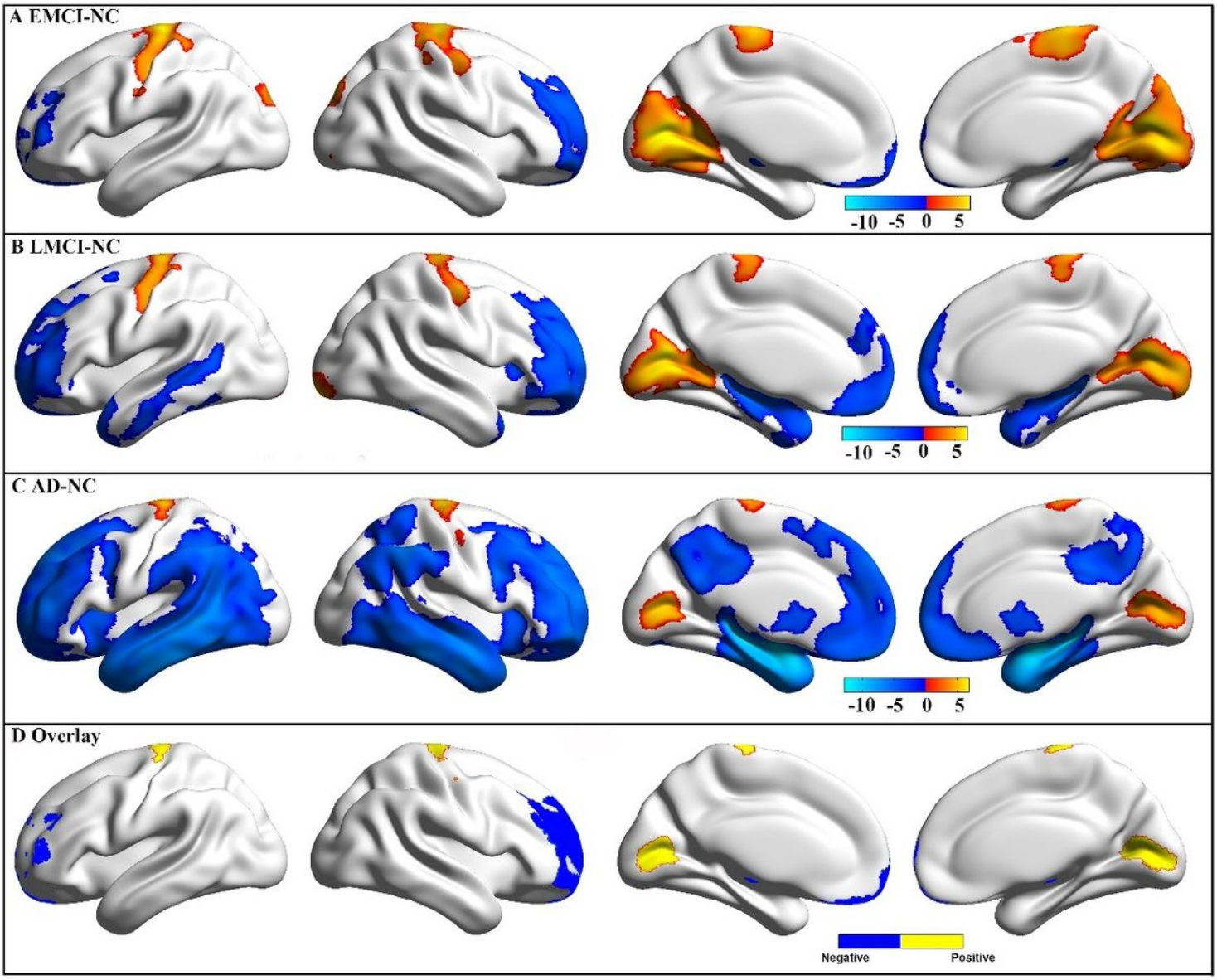

Figure 2

GMV difference for EMCI (A), LMCI (B), and AD (C) patients as compared to NC. The results were obtained using two sample t tests and were corrected using Gaussian random field (GRF, a cluster level of $p < 0.05$ and a voxel level of $p < 0.001$). The color bar represents t -values and a positive t -value (warm color) indicates increased GMV in this group as compared to NC. Negative and positive (D) overlap among three groups.

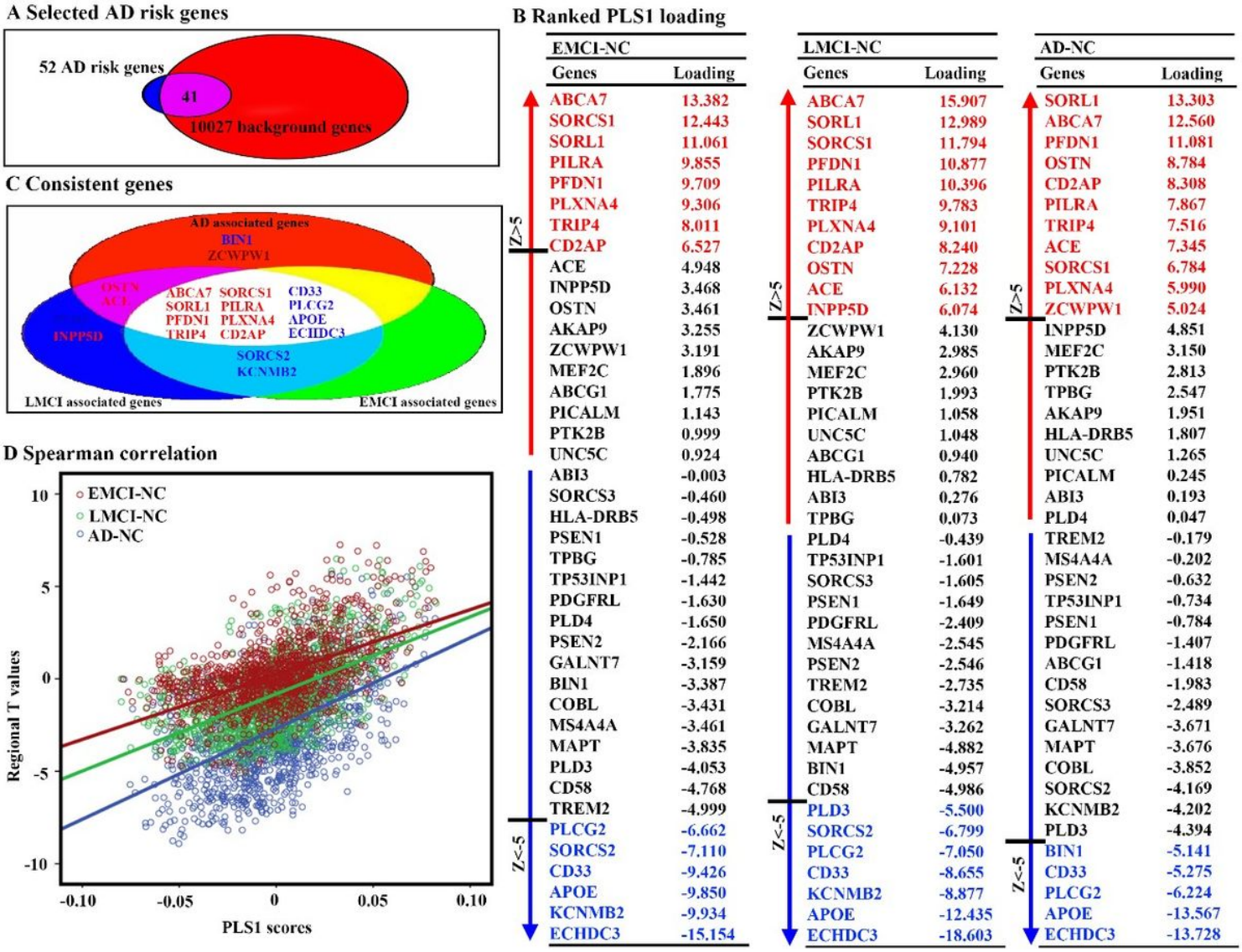

Figure 3

Gene expression level related to regional GMV differences using PLS. (A) Forty one genes were selected as interested genes. (B) Ranked PLS1 loadings for 41 selected AD risk genes. Z>5 and Z<-5 were considered as significant. (C) Twelve consistent genes among three groups, including 8 positively associated genes, and 4 negatively associated genes. (D) Scatterplots of regional PLS1 scores and regional changes of GMV. PLS1: the first component of PLS.

R values

Genes	EMCI-NC	LMCI-NC	AD-NC
ABCA7	0.280	0.304	0.259
SORCS1	0.295	0.300	0.153
SORL1	0.313	0.339	0.311
PILRA	0.228	0.219	0.168
PFDN1	0.268	0.304	0.287
PLXNA4	0.235	0.225	0.143
TRIP4	0.215	0.242	0.192
CD2AP	0.164	0.203	0.210
CD33	-0.190	-0.164	-0.103
PLCG2	-0.139	-0.159	-0.147
APOE	-0.235	-0.296	-0.285
ECHDC3	-0.425	-0.499	-0.403

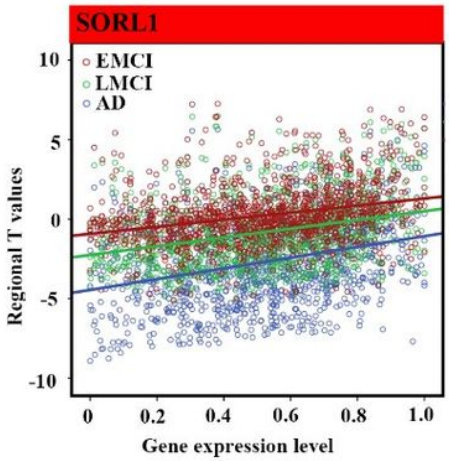

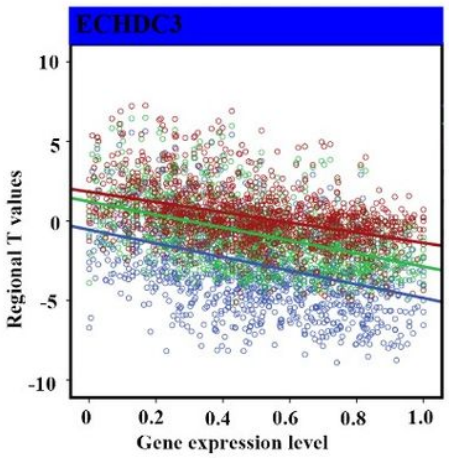

Figure 4

Spearman correlations between gene expression levels of overlap genes and regional GMV difference of EMCI, LMCI, and AD patients compared to NC. Blue font represents for negative association and red for positive association.

	cEMCI-NC		sEMCI-NC		cLMCI-NC		sLMCI-NC	
Genes	PLS1	R values	PLS1	R values	PLS1	R values	PLS1	R values
ABCA7	12.667	0.239	13.250	0.278	13.799	0.293	13.802	0.298
SORCS1	10.810	0.217	12.566	0.311	11.095	0.262	10.839	0.314
SORL1	8.165	0.240	11.973	0.327	12.868	0.344	13.298	0.301
PILRA	10.854	0.209	9.225	0.220	9.667	0.205	9.878	0.227
PFDN1	6.404	0.184	10.507	0.283	11.070	0.304	11.306	0.279
PLXNA4	7.120	0.195	10.014	0.244	8.459	0.203	8.179	0.234
TRIP4	8.629	0.196	7.551	0.205	8.657	0.223	8.666	0.243
CD2AP	6.386	0.140	6.625	0.165	8.199	0.210	8.752	0.176
CD33	-11.351	-0.206	-7.969	-0.175	-7.383	-0.141	-7.097	-0.188
PLCG2	-7.159	-0.107	-6.644	-0.153	-7.139	-0.159	-6.958	-0.149
APOE	-8.936	-0.185	-9.880	-0.240	-13.004	-0.303	-13.192	-0.270
ECHDC3	-14.868	-0.343	-14.708	-0.437	-15.944	-0.473	-16.488	-0.470

Figure 5

PLS1 scores and Spearman correlations between gene expression levels of overlap genes and regional GMV difference of cEMCI, sEMCI, cLMCI, and sLMCI patients compared to NC. Blue font represents for negative association and red for positive association.

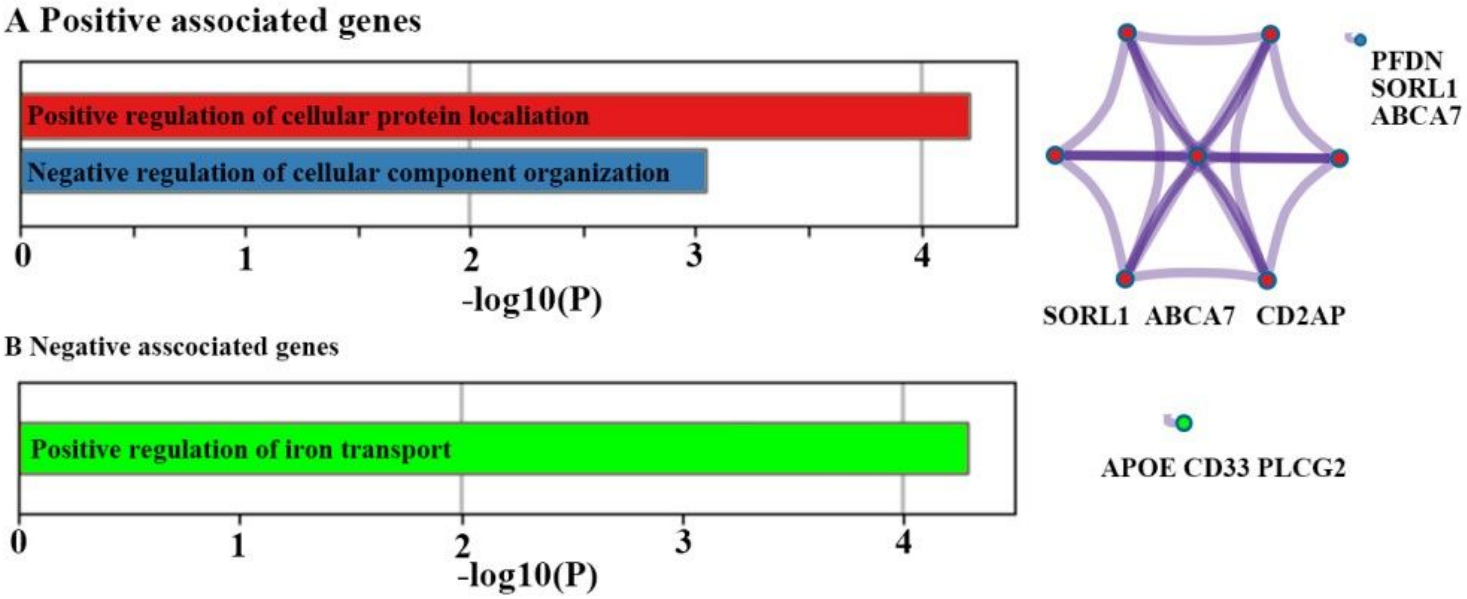

Figure 6

Functional enrichment analyses. Ontology terms and Metascape enrichment network visualization for positive (A) and negative (B) associated genes. The size of the circle represents the number of genes involved in a given term. Each term is represented by a circle node, where its size is proportional to the number of input genes included in that term, and its color represents its cluster identity.